Modeling of Hydrocarbon Redeposition in the Gaps of Castellated Structures

K. Ohya 1), K. Inai 1), Y. Kikuhara 1), A. Ito 2,3), H. Nakamura 3), Y. Tomita 3), G. Kawamura 3), T. Tanabe 4)

1) The University of Tokushima, Tokushima 770-8506, Japan
2) Nagoya University, Nagoya 464-8602, Japan
3) National Institute for Fusion Science, Toki 509-5292, Japan
4) Kyushu University, Fukuoka 812-8581, Japan

e-mail: ohya@ee.tokushima-u.ac.jp

Abstract. Castellated armor tiles are anticipated to withstand intense heat fluxes on the first wall and the divertor area in ITER. However, there is a critical issue of fuel (tritium) retention and impurity transport in the gaps between the castellated tiles. In this study, we have performed a simulation calculation of transport and deposition of hydrocarbons on the castellated structure in order to understand the mechanisms of co-deposition and to mitigate carbon deposition in the gaps by changing castellated geometry. Reflection/sticking coefficients of the tile surface in realistic conditions were investigated by using molecular dynamics (MD) of collisions with all hydrocarbons that result from chemical sputtering. Furthermore, we have incorporated a particle-in-cell (PIC) simulation into the hydrocarbon transport code for detailed discussion of the redeposition characteristics of the castellated tile. A new castellation geometry of unit cells with a tilted surface is proposed and the optimization of the shape of the cell is very likely to work to minimize the redeposition rate in the gaps. The tile geometry is important to reduce the in-vessel tritium inventory for the safety operation of fusion reactors.

1. Introduction

In present large tokamaks, most of hydrogen isotopes are retained in the carbon deposition layers on the plasma shadowed area and the tile gaps in the divertor. Plasma wall interaction of the hydrogen isotope plasma with carbon based wall components leads to chemical erosion processes, resulting in hydrocarbon impurities. Transport of hydrocarbons is most important mechanism of the hydrogen isotope retention. Castellated armor tiles are of acute interest to ensure thermo-mechanical durability for the first wall and divertor of ITER. However, the introduction of castellated structures imposes serious concerns on the impurity accumulation and the tritium retention in gaps between the unit cells, because of the difficulty of removal from the gaps. Dedicated studies addressing the performance of castellated structures under plasma exposure are ongoing on several tokamaks [1-3]. Series of experimental investigations with ITER-like castellated limiter with rectangular and roof-like shaped cells along with modeling were performed in TEXTOR [4] and the roof-like cells made significant asymmetry of carbon deposition distribution between plasma-open and plasma-shadowed sides in the gaps [5].

A Monte Carlo simulation code, EDDY, which we have developed, allows us to perform a self-consistent calculation of impurity release and material mixing of a wall surface with

transport of released atomic and hydrocarbon impurities in the plasma [6]. Recent EDDY calculation of erosion and deposition in the gaps reproduced the asymmetric distribution on the roof-like cells [7]. Furthermore, the small tilt (~a few degrees) of the cells against the toroidal direction minimized the amount of redeposition in the gaps and a new castellation geometry with the cells tilted against both poloidal and toroidal directions were proposed. However, the plasma profile in the vicinity of the surface is affected by the gap structure and by the angle of the magnetic field against the cell surface. In this study, we have incorporated a particle-in-cell (PIC) simulation into the EDDY code calculation for detailed discussion of the redeposition characteristics of the gaps in the castellated tile.

The hydrocarbons released due to chemical sputtering of the carbon walls are dissociated into different neutral and ionized products in the plasma and the particles returning to the surface can stick (redeposit) or move back (reflect) into the plasma. The surface reaction is one of critical mechanisms for long-distance transport of the carbon/hydrocarbon impurities in the present large tokamaks. In this study, a classical molecular dynamics (MD) simulation is applied to evaluate the hydrocarbon interaction with the surface in fusion-relevant conditions, and the calculated reflection/sticking coefficients and the distribution of reflected species are used for simulation of hydrocarbon transport and its redeposition on the castellated surfaces.

2. Monte Carlo (MC) Simulation of Hydrocarbon Transport in Plasmas

Figure 1 show a schematic view of the castellated tile with the cells tilted against both toroidal and poloidal directions, along with the conventional configuration (Fig. 1(a)). In order to hide both of the toroidal and poloidal gaps from direct access of the plasma, the gaps are rotated by 45^{o} against the magnetic field lines. A homogeneous plasma with constant plasma temperature and the density contacts the top surface of the tile; the ion and electron temperatures are assumed to be equal to each other. The rectangular volume above a cell (including gaps) is the simulation volume, the sides of which have periodic boundary conditions. The thickness of the plasma is 10 cm. Hydrocarbons, such as methane (CH_4) and ethane (C_2H_6), with a Maxwllian velocity distribution corresponding to a temperature of 0.1 eV are generated randomly from plasma-open areas of the top surface. The angle of magnetic field lines against the surface of the conventional structure is 5^{o} and the magnetic field strength is 5 T. The released hydrocarbons experience complex collision reactions in the plasma distributed on the tile surface and in the gaps, the density and potential distributions of which are calculated by using a PIC code (see the next section). The electron-impact ionization and dissociation, dissociative recombination of ionized hydrocarbons, and charge exchange by hydrogen ions, including the dissociation, are followed using atomic data package from Janev/Reiter [8]. When a particle produced by the reaction is charged, as described in [9], it gyrates in the magnetic field and experiences friction force parallel to the

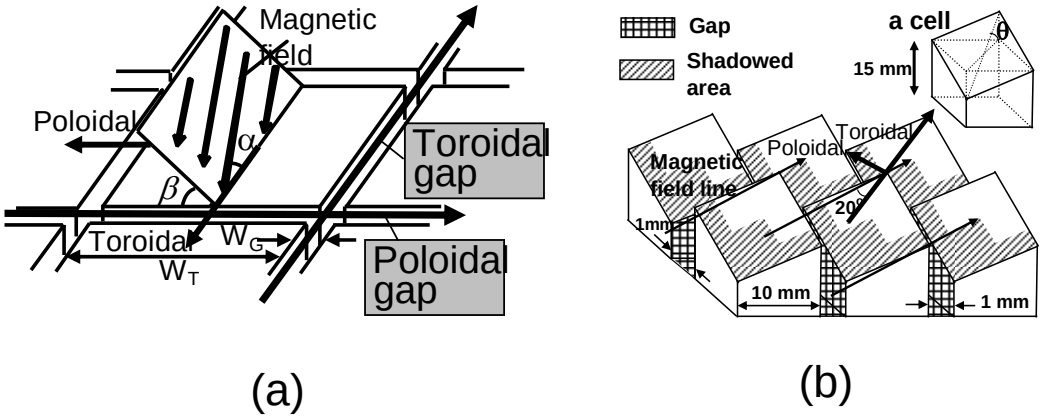

FIG. 1. (a) Schematic view of the configuration of the castellated tiles and (b) a castellated tile with the cells tilted against both toroidal and poloidal directions.

magnetic field lines, cross-field diffusion, acceleration by the electric field in the plasma sheath. In the simulation volume, constant plasma temperature is assumed so that thermal gradient force is not taken into account. The particles returning to the surface can either stick (redeposit) or move back (reflect) into the plasma as different types of hydrocarbons, according to the emission probability for each hydrocarbon calculated by using a MD code described later.

3. Particle-In-Cell (PIC) Plasma Simulation in Gaps and Simple Model for Plasma Sheath on Tilted Surface and in the Gaps

In order to simulate the magnetic presheath and Debye sheath formed at the boundary between a scrape-off layer (SOL) plasma and a wall surface, we have developed a two dimensional kinetic code with three dimensions in velocity space. Furthermore, since the magnetic field lines are inclined against the surface normal, the gyro-motion of the ions is taken into account. Fully ionized magnetized plasma with one species of singly charged ions bombards a perfectly absorbing and electrically floating wall. The electric field at the surface is determined by the charge density on the surface. The PIC code is based on the integrations of the equation of motion and of Poisson's equation to obtain the self-consistent electric field that accelerates the ions. For the ions, we use half-Maxwellian with velocity cut-off only in the direction of magnetic field that satisfies the generalized Bohm criterion at the electrostatic sheath entrance, whereas the electrons are assumed to be Maxwellian. The effective temperature of ion is varied with the cut-off velocity, $v_{ci} = 0.6 \times \sqrt{T_i / m_i}$ [10].

Since the PIC simulation is very time consuming to evaluate the sheath structure on all of the shaped surfaces of the castellated tile, the sheath on the tilted surfaces between the gaps is simplified by an analytical sheath model. For this purpose, the Brooks model [11] is used

with following modification: $\phi(r)=\phi_0\exp[-l/\lambda]$, where $\lambda=\delta_1\sin\beta\lambda_L+\delta_2(1-\sin\beta)\lambda_D$ and $\phi_0=-3k_BT_e$. β is the angle of the magnetic field line from the surface normal, λ_L is gyro-radius of the plasma ion, λ_D is the Debye length, δ_1 and δ_2 are the arbitrary constants, and l is the distance from the surface. The decay of the plasma density is assumed to be dependent on the sheath potential according to the Boltzmann relation.

4. Molecular Dynamics (MD) Simulation of Collisions of Hydrocarbons with Surfaces

Not only the reflection coefficients or sticking coefficients of plasma facing walls but also emission species of hydrocarbons are calculated according to a classical MD scheme. We also prepared fusion-relevant C and W surfaces, including hydrogenated amorphous carbon and and W-C mixed surfaces by the MD code. We used the interaction potential based on analytic bond-order scheme, which was developed for the ternary system W-C-H by Juslin et al. [12]. Atomistic trajectories in a temperature-controlled simulation cell are followed using a variable-time-step velocity Verlet algorithm [13]. The temperature control of the material used a Langevin thermostat with a time constant of 0.1 ps at a temperature of 300 K, in order to dissipate the excess heat between impacts. The atoms of the bottom surface are held fixed, which prevents the entire substrate from moving downward when bombarded by energetic atoms. The top surface is free, and the sides of the cell have periodic boundary conditions.

As found in the present fusion devices, the wall surface that is bombarded is not static, but is modified by the plasma injection. When a W surface is bombarded by C ions with the energies of several tens of eV or more, the surface is eroded but some C ions are implanted in the surface layer of W. In order to prepare a W-C mixed layer, a W crystalline cell comprised 10 x 10 x 20 unit cell was bombarded by 100 eV C ions with the fluence of $5\text{x}10^{16}$ cm^{-2} along [001]. Since the bombardment by low-energy (10eV) C ions with the fluence of $5\text{x}10^{16}$ cm^{-2} results in the formation of amorphized C layer on W, the hydrogen uptake in the amorphous C was followed by simultaneous bombardment with 0.025 eV C and 0.1 eV-30 eV H with the total fluence of $2\text{x}10^{16}$ cm^{-2}; where the hydrogen concentration in the layer is varied with the impact energy of H.

Since the impact position and molecule direction of an incident particle clearly influence whether it reflects from or sticks on the surface, 100 particles for each hydrocarbon, i.e. CH_x (x=0-4) and C_2H_x (x=0-6), with random direction are landed at random position of the top surface. The incident angle is 45^o against the surface normal.

5. Hydrocarbon Reflection and Sticking on Fusion-Relevant Surfaces

The calculated reflection coefficients for different hydrocarbons and different surface conditions are summarized in Fig. 2. Due to the break-up of incident hydrocarbons, many different dissociation products are released from the surfaces, however, all species of CH_x (or

C_2H_x) are summed in the figures. With increasing hydrogen content (i.e. x) of incident hydrocarbon, the reflection coefficient increases, whereas with increasing impact energy, the coefficient decreases (Figs. 2(a) and 2(b)). Heavy hydrocarbons (C_2H_y) are reflected more due to smaller velocity in the condition of constant impact energy. On the other hand, carbon atoms and carbon molecules can easily stick hydrogenated amorphous C layer formed on the plasma facing walls. Mixed amorphous layers formed due to the erosion and redeposition process in the present devices, such as amorphous C and W-C mixed layers, decrease the reflection coefficient of C and W crystalline surfaces (Fig. 2(c)). Furthermore, hydrogen uptake in amorphous C decreases the coefficient more. Figure 2(d) demonstrates that the emission probability of CH_x (x=0-4) for the incidence of CH_4 is enhanced with increasing areal density of hydrogen in amorphous C. In this study, the hydrogen density was changed due to the change in the impact energy of hydrogen in preparation of the starting surface (see the insets of the figure).

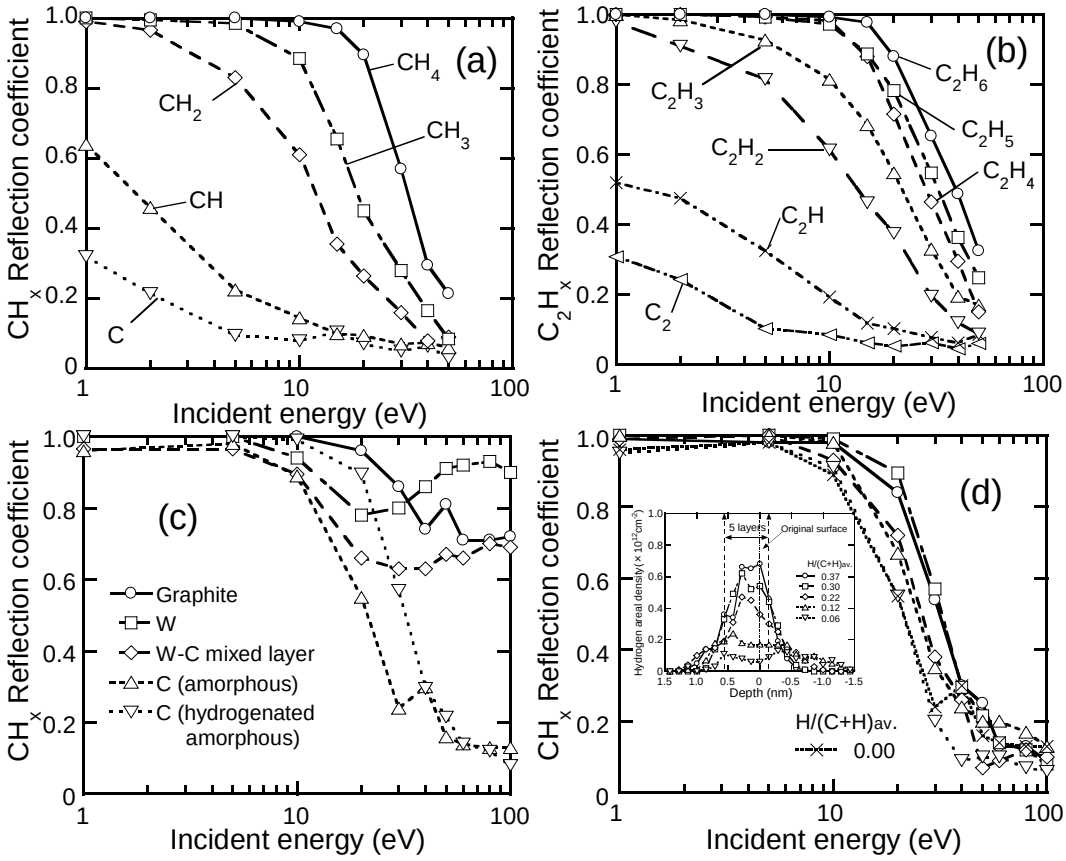

FIG. 2. Reflection coefficients of hydrogenated amorphous carbon for (a) CH_x (x=0-4) and (b) C_2H_x (x=0-6), and reflection coefficients of (c) different material surfaces for CH_4, and (d) hydrogenated amorphous carbon layer as a function of the amount of hydrogen in the layer.

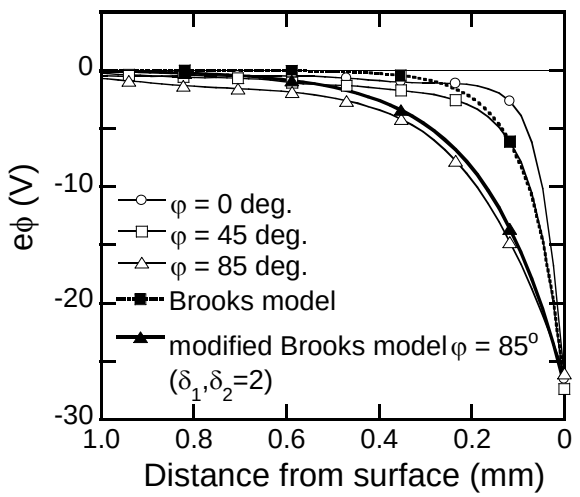

FIG. 3. Sheath potential distribution for different angles of magnetic field lines with respect to the surface normal.

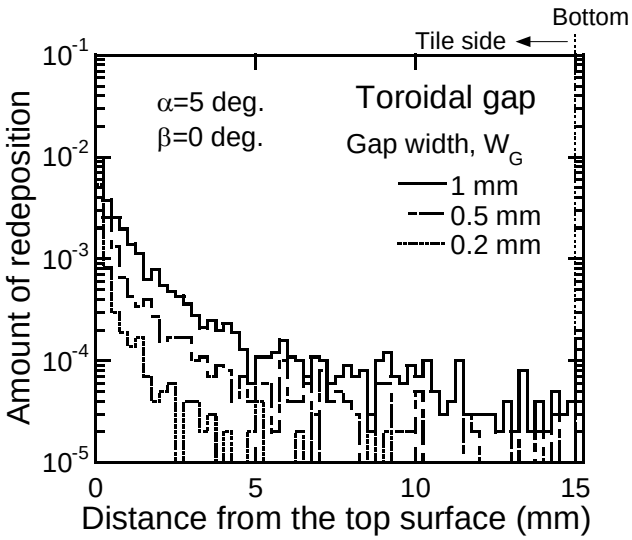

FIG. 4. Amount of redeposition on the side of the toroidal gap with different widths as a function of the distance from the top edge of the conventional castellated tile.

6. Influence of Plasma and Sheath in Gaps on Hydrocarbon Redeposition

The sheath potential distribution on a flat surface is shown in Fig. 3, for different magnetic angles at the plasma electron temperature of 10 eV and the density of 10^{18} m^{-3}, and the magnetic field strength is 5 T. When the magnetic field approaches parallel to the surface, the width of magnetic presheath becomes lager since it is roughly proportional to the gyro-radius of the thermalized ions. Although the potential distribution for the original Brooks model decays faster than for the PIC calculation at glancing angle of 85^{o}, the present modification of the model results in a reasonable agreement with the PIC distribution.

The redeposition distribution of hydrocarbon on the sides of the poloidal gap on a conventional castellated tile with flat cell surface is as a function of the gap width, as shown in Fig. 4 where the plasma temperature and density are 10 eV and 10^{18} m^{-3}; B=5T. When the width of the gap is 1 mm and 0.5 mm, the redeposition can be found at the bottom of the gap, the bottom of which is 15 mm. On the other hand, a very narrow gap (0.2 mm) causes the redeposition to localize near the gap edge.

7. Castellation Structures with Tilted Cells for Reduction of Hydrocarbon Redeposition in Gaps

Such calculations of the redeposition in the gap are applied to the castellated tile with cells tilted in both toroidal and poloidal directions. The typical results are shown in Fig. 5 as a function of the tilt angle for the same conditions as Fig. 4. Nevertheless, the magnetic field

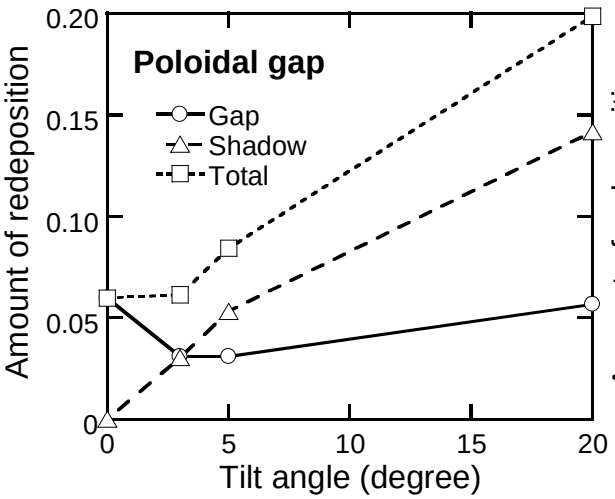

FIG. 5. Amount of redeposition on the gap sides, the shadowed area on the top surface and the whole region, as a function of the tilt angle of the cells in the castellated tile.

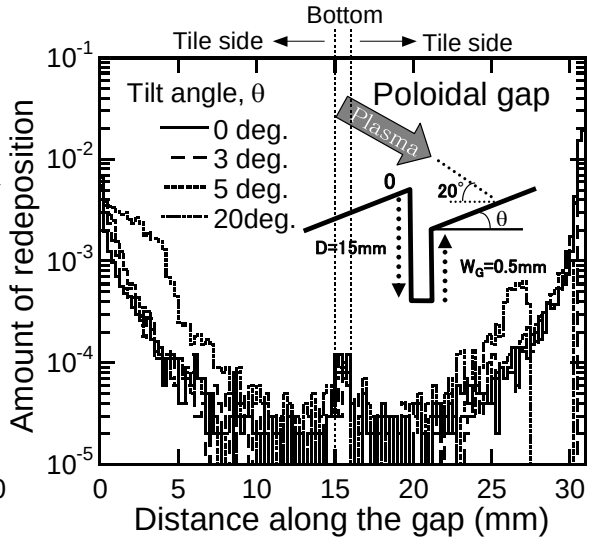

FIG. 6. Redeposition distribution in the poloidal gap of the caltellated tile for different tilt angles. The distance is measured from the top edge of the plasma-shadowed side towards that of the plasma-open side. The bottom of the gap is between 15 mm and 16 mm.

lines are inclined by 20^o from the surface of the un-tilted cells ($\theta=0^o$). Because of small tilt of the unit cell, the amount of redeposition per launched hydrocarbon (CH_4) is suppressed in the gap. This is a clear evidence that the gap in this particular geometry is hidden from direct access of launched hydrocarbons. With further increasing the tilt angle of θ, the redeposition in the gap is hidden by the redeposition on the shadowed area of the top surface of the cell. Therefore, reduction of the areas directly exposed to plasmas with the optimization of the shape of the castellated unit cell is very likely to work to minimize the amount of redeposition in the gaps of the castellated structure, e.g., at the angle of $\theta=2^o\sim3^o$.

Figure 6 shows the redeposition distribution on the whole area in the poloidal gap with the gap width of 1 mm. The edges in the plasma-shadowed and plasma-open sides for un-tilted cells ($\theta=0^o$) are 0 mm and 31 mm, respectively. Since the re-erosion of the redeposits is not taken into account, the amount of redeposition is larger for the plasma-open edge than for the plasma-shadowed edge. The redeposition on the plasma-open side is suppressed due to the tilt of the top surface of the cells, although for large tilt angle ($\theta=20^o$) the redeposition on the plasma-shadowed side is enhanced due to additional deposition of hydrocarbons reflected from the top surface of the cells.

8. Concluding Remarks

For understanding the redeposition characteristics in gaps between the unit cells of

castellated armor tiles, transport and redeposition of hydrocarbons released by chemical sputtering are simulated by a Monte Carlo simulation code, EDDY. The simulation with fidelity requires not only exact cross sections for complex reactions of the hydrocarbons in plasmas but also reflection and sticking probabilities of plasma facing walls for the break-up products that result from the plasma reactions. To evaluate reflection probabilities of hydrocarbons on fusion-relevant C and W, a classical molecular dynamics (MD) code is developed where hydrogenate amorphous C and W-C mixed layers are prepared by pre-bombardment of C and H ions. Mixed amorphous layers decrease the reflection coefficient of C and W. Hydrogen uptake in the layers decreases the coefficient further more. Since plasma profile above tile surfaces is affected by the gap between the cells, a particle-in-cell (PIC) code is developed to incorporate into the EDDY code simulation. When the gap width is 0.5 mm or more, the redeposition can be found at the bottom of the gap, whereas very narrow gap (<0.2 mm) causes the redeposition to localize at the gap edge. A new geometry of the unit cell, the surface of which is tilted by 2^{o}~3^{o} against both toroidal and poloidal directions was ensured to hid both the toroidal and poloidal gaps from direct access of the plasma ions.

Acknowledgement

This work was supported by KAKENHI (19055005).

References

[1] KRIEGER, K., et al., J. Nucl. Mater. 363-365 (2007) 870.
[2] WONG, C., et al., J. Nucl. Mater. 363-365 (2007) 276.
[3] RUDAKOV, D., et al., Phys. Scr. T 128 (2007) 29.
[4] LITNOVSKY, A., et al., J. Nucl. Mater. 337-339 (2005) 917; 363-365 (2007) 1481.
[5] LITNOVSKY, A., et al., Phys. Scr. T128 (2007) 45; J. Nucl. Mater. 000 (2008) 000.
[6] OHYA, K., Phys. Scr. T124 (2006) 70.
[7] INAI, K, OHYA, K., et al., Contrib. Plasma Phys. 48 (2008) 275; 18th Intern. Conf. on Plasma Surface Interactions, P2-09, May 26-30, 2008, Toledo, Spain.
[8] JANEV, R.K., REITER, D., Rep. Forscnungszentrum Jülich, Jül-3966 (2002) and Jül-4005 (2003).
[9] INAI, K., OHYA, K., Jpn. J. Appl. Phys. 46 (2007) 1149.
[10] KAWAMURA, G., FUKUYAMA, A., Phys. Plasmas 14 (2007) 083502.
[11] BROOKS, J.N., Phys. Fluids 25 (1990) 1858.
[12] JUSLIN, N., et al., J. Appl. Phys. 98 (2005) 123520.
[13] INAI, K., KIKUHARA, Y., OHYA, K., Surf. Coat. Technol. 202 (2008) 5374.